Drug Design, Development and Therapy

Dovepress
open access to scientific and medical research

Open Access Full Text Article

ORIGINAL RESEARCH

Functional characterization of a competitive peptide antagonist of p65 in human macrophage-like cells suggests therapeutic potential for chronic inflammation

This article was published in the following Dove Press journal:
Drug Design, Development and Therapy
3 December 2014
Number of times this article has been viewed

Mythily Srinivasan[1]
Corinne Blackburn[1]
Debomoy K Lahiri[2,3]

[1]Department of Oral Pathology, Medicine and Radiology, Indiana University School of Dentistry, [2]Institute of Psychiatry Research, Department of Psychiatry, [3]Department of Medical and Molecular Genetics, School of Medicine, Indiana University-Purdue University, Indianapolis, IN, USA

Abstract: Glucocorticoid-induced leucine zipper (GILZ) is a glucocorticoid responsive protein that links the nuclear factor-kappa B (NFκB) and the glucocorticoid signaling pathways. Functional and binding studies suggest that the proline-rich region at the carboxy terminus of GILZ binds the p65 subunit of NFκB and suppresses the immunoinflammatory response. A widely-used strategy in the discovery of peptide drugs involves exploitation of the complementary surfaces of naturally occurring binding partners. Previously, we observed that a synthetic peptide (GILZ-P) derived from the proline-rich region of GILZ bound activated p65 and ameliorated experimental encephalomyelitis. Here we characterize the secondary structure of GILZ-P by circular dichroic analysis. GILZ-P adopts an extended polyproline type II helical conformation consistent with the structural conformation commonly observed in interfaces of transient intermolecular interactions. To determine the potential application of GILZ-P in humans, we evaluated the toxicity and efficacy of the peptide drug in mature human macrophage-like THP-1 cells. Treatment with GILZ-P at a wide range of concentrations commonly used for peptide drugs was nontoxic as determined by cell viability and apoptosis assays. Functionally, GILZ-P suppressed proliferation and glutamate secretion by activated macrophages by inhibiting nuclear translocation of p65. Collectively, our data suggest that the GILZ-P has therapeutic potential in chronic CNS diseases where persistent inflammation leads to neurodegeneration such as multiple sclerosis and Alzheimer's disease.

Keywords: glucocorticoid-induced leucine zipper, therapeutic potential, translational impact, chronic inflammation

Correspondence: Mythily Srinivasan
Oral Pathology, Radiology and Medicine, Indiana University School of Dentistry, 1121 West Michigan St, Indianapolis, IN 46202, USA
Tel +1 317 278 9686
Fax +1 317 278 3018
Email mysriniv@iupui.edu

Debomoy K Lahiri
Department of Psychiatry, Indiana University School of Medicine, Institute of Psychiatric Research, 791 Union Drive, Indianapolis, IN 46202, USA
Tel +1 317 274 2706
Fax +1 317 274 1365
Email dlahiri@iupui.edu

Introduction

Persistent inflammation is widely recognized as a common denominator in the pathogenesis of multiple diseases with diverse clinical manifestations, such as immune-mediated rheumatoid arthritis or multiple sclerosis and neurodegenerative Alzheimer's disease or Parkinson's disease.[1–5] Sustained or unregulated activation of the transcription factor nuclear factor kappa B (NFκB) is integral to the persistence of inflammation.[6,7] The most common form of NFκB is a heterodimer of p50 and p65 subunits. In resting cells, NFκB exists in the cytoplasm as an inactive complex bound to IκB inhibitory proteins.[2,8] Activation of NFκB signaling induces proteolytic degradation of IκB inhibitory proteins, releasing the p50 and p65 subunits. p65 is the functionally dominant subunit that, upon release from the inhibitory complex, translocates to the nucleus, where it binds cognate NFκB binding sites in the DNA and modulates expression

© 2014 Srinivasan et al. This work is published by Dove Medical Press Limited, and licensed under Creative Commons Attribution – Non Commercial (unported, v3.0) License. The full terms of the License are available at http://creativecommons.org/licenses/by-nc/3.0/. Non-commercial uses of the work are permitted without any further permission from Dove Medical Press Limited, provided the work is properly attributed. Permissions beyond the scope of the License are administered by Dove Medical Press Limited. Information on how to request permission may be found at: http://www.dovepress.com/permissions.php

of several genes involved in apoptosis, and immune and inflammatory responses.[2,7]

Mechanistically, many drugs used in the treatment of chronic inflammatory pathologies act at least in part by inhibiting NFκB transactivation. For example, the effects of many of the nonsteroidal anti-inflammatory drugs are mediated by suppression of NFκB activation by inhibiting the IκB complex or by activation of peroxisome proliferator-activated receptor gamma, a negative regulator of NFκB transcription.[2,9] The profound anti-inflammatory effects of the widely-used glucocorticoids[10] as well as the therapeutic efficacy of many currently approved biologics has been attributed to indirect inhibition of NFκB signaling.[11,12] However, nonspecific responses, serious adverse effects, and/or high cost are some of the factors that compromise long-term use of these therapeutic agents.

Interactome analysis using MetaCore™ (Thomson Reuters, New York, NY, USA) identified glucocorticoid-induced leucine zipper (GILZ) as a "divergence" hub functionally linked to multiple proteins in the NFκB and glucocorticoid signaling pathways.[13] GILZ was identified originally during systematic study of genes transcriptionally induced by glucocorticoids.[14,15] Functionally, GILZ has been shown to suppress immune responses by preventing signaling via AKT or PKB (protein kinase B)/Ras proteins, inhibiting cyclooxygenase -2 (Cox-2) activity, and skewing proinflammatory cytokine(interferon gamma [IFN-γ], tumor necrosis factor alpha [TNF-α]) responses to anti-inflammatory cytokine (interleukin [IL]-10, transforming growth factor beta [TGF-β]) responses.[16–19] Mechanistically, the inhibitory potential of GILZ is attributed to its ability to bind and prevent nuclear translocation of p65, thereby inhibiting transactivation of pathological mediators.[16,20] Indeed, it is suggested that the profound therapeutic efficacy of glucocorticoids could be attributed to the induced upregulation of GILZ.[21,22]

Structurally, GILZ has an amino terminal-dimerizing leucine zipper motif and a proline-rich carboxy terminus (Figure 1A). Mutational analysis suggested that the p65 binding domain of GILZ is localized in the proline-rich region of its carboxy terminus.[20,23] In the eukaryotic proteome, proline-rich regions are widely represented in the interfaces of transient protein-protein interactions and are considered attractive targets for drug development.[24,25] A common strategy in the discovery of peptide drugs involves exploitation of the complementary surfaces of the naturally occurring binding partners.[26] We observed that a synthetic peptide (GILZ-P) derived from the proline-rich region of GILZ suppressed immune-mediated inflammatory responses in mice.[27] Kinetic analysis suggested

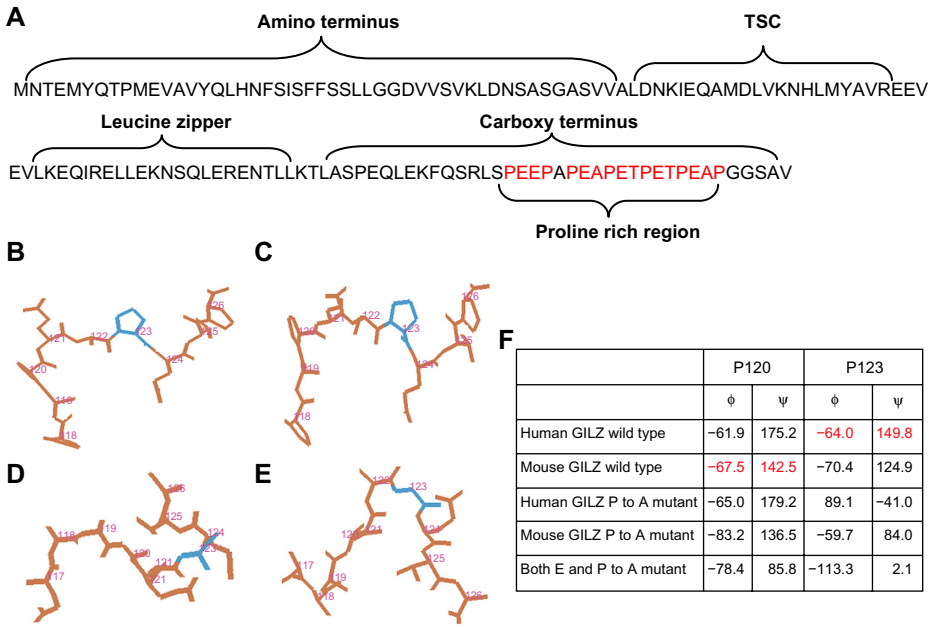

F

	P120		P123	
	ϕ	ψ	ϕ	ψ
Human GILZ wild type	−61.9	175.2	−64.0	149.8
Mouse GILZ wild type	−67.5	142.5	−70.4	124.9
Human GILZ P to A mutant	−65.0	179.2	89.1	−41.0
Mouse GILZ P to A mutant	−83.2	136.5	−59.7	84.0
Both E and P to A mutant	−78.4	85.8	−113.3	2.1

Figure 1 The GILZ protein and peptide.
Notes: (**A**) Primary structure of human GILZ showing different domains. The proline-rich region with "PXXP" motifs is highlighted. Homology models of (**B**) mouse or (**C**) human GILZ using porcine δ sleep-inducing peptide (PDB: 1DIP) as the template are shown. The proline in helical poly-l-proline type II conformation is shown in blue. Models of GILZ mutants are shown with (**D**) alanine substitution of proline residues or (**E**) both proline and glutamic acid residues in the proline-rich region. The alanine substituting the poly-l-proline type II helical proline is shown in blue. (**F**) Table showing the ψ and ϕ dihedral angles of potentially critical proline residues in the carboxy terminus of the human and mouse GILZ models and the indicated mutants.
Abbreviations: GILZ, glucocorticoid-induced leucine zipper; TSC, TGF-beta stimulated clone-box.

the strength of interaction between the GILZ and the p65 proteins to be in micromolar concentrations consistent with observations in transient intermolecular interactions.[27,28] In this study, we characterized the secondary structure of GILZ-P, investigated its toxicity, and evaluated its functional potential in human macrophage-like THP-1 cells.

Materials and methods

Peptides and preparation of Pep-1:peptide complexes

GILZ-$P_{115–137}$ (Figure 1B) and control peptides (Control-P) of scrambled residues were synthesized as peptide amides with amino terminal acetylation. All peptides were 95% pure by mass spectrometry. Intracellular delivery of GILZ-P and Control-P was achieved using the Pep-1 chariot reagent (Active Motif, Carlsbad, CA, USA). Immediately prior to each experiment, a noncovalent complex of the chariot and peptide drug was formed by combining Pep-1 and GILZ-P or Control-P at appropriate concentrations in 100 µL of sterile phosphate-buffered saline and incubating at room temperature for 30 minutes.[29] The noncovalent complex of Pep-1 with GILZ-P and Control-P will henceforth be referred to as GILZ-P_c or Control-P_c.

Circular dichroism

Circular dichroism (CD) spectra were collected on a MOS450 AF/CD spectrometer (Bio-Logic Science Instruments , Clarix, France) at 25°C in the 190–270 nm wavelength range with a 0.5 nm resolution and a scan rate of 200 nm per minute. The samples were prepared by dissolving lyophilized GILZ-P and Control-P at a 100 µM concentration in citrate buffer (1 mM sodium citrate, 1 mM sodium borate, 1 mM sodium phosphate, 15 mM NaCl) with pH adjusted at 7.0. Each spectrum was measured five times with individually prepared solutions. Raw CD signals were converted to mean residue molar ellipticity $(\theta)_{MRW}$ in degrees cm^2/dmol using the formula $[\theta]_{MRW} = [\theta]_{obs}/10\,l\,c\,n$, where $[\theta]_{obs}$ represents the observed ellipticity, l is the path length in centimeters, c is the molar concentration of peptide, and n is the number of residues in the peptide. To determine 0% polyproline type II (PPII) helical content, CD spectra were recorded with GILZ-P and Control-P dissolved in 6 M $CaCl_2$.[28] The data used for graphical presentation and analyses were each an average of five different scans.

Cell cultures

The human monocytic cell line, THP-1 (a gift from Dr Michael Klemsz, Department of Immunology, Indiana University School of Medicine, Minneapolis, IN, USA) was maintained in complete Roswell Park Memorial Institute (RPMI)-1640 medium (Sigma-Aldrich, St Louis, MO, USA) supplemented with 1% L-glutamine, 5 mM β-mercaptoethanol, and 10 mM N-(2-Hydroxyethyl)piperazine-N'-(2-ethanesulfonic acid) (HEPES) (Life Technologies, Carlsbad, CA, USA), with 10% heat-inactivated fetal calf serum, 100 U/mL penicillin, and 100 µg/mL streptomycin, and seeded in 75 cm^2 flasks at a density of 5×10^6 cells per flask. The cells were cultured in 5% CO_2 atmosphere at 37°C , and the medium was changed every 2–3 days.[30] For differentiation to mature macrophages, cultured THP-1 cells were initially rested for 24 hours in fresh medium without antibiotics. Next, the cells were seeded at 5×10^5 cells/mL in a new 75 cm^2 flask and stimulated with 200 nM of phorbol-12 myristate 13-acetate (PMA; Sigma-Aldrich) for 72 hours.[31] Previously, PMA has been shown to induce THP-1 cells to differentiate into mature human macrophages.[31–33] The differentiation was confirmed by flow cytometric analysis for expression of the macrophage-specific markers, CD14 and CD11c. The cells were then washed to remove PMA and rested in fresh complete RPMI-1640 medium for 24 hours prior to use in experiments.[31,32]

Cell viability and apoptosis assays

THP-1 cells (1×10^6/mL) suspended in complete RPMI-1640 were incubated in the presence of medium-alone or increasing concentrations of GILZ-P_c (10–640 µM) in a 5% CO_2 incubator at 37°C. The viability of cells harvested at 1, 4, 8, 12, 24, and 48 hours was determined by trypan blue exclusion using a Countess automated cell counter (Thermo Fisher Scientific, Waltham, MA, USA).[34] Adherent cells were treated with 0.5 mL of 0.05% trypsin-0.5 mM ethylenediaminetetraacetic acid (EDTA) (Thermo Fisher Scientific) at 37°C for approximately 5 minutes to enhance removal. In separate experiments, THP-1 macrophages cultured similarly were harvested at different time points and stained with Annexin V and propidium iodide using the Annexin-V-FLUOS staining kit (Roche Diagnostics, Indianapolis, IN, USA) according to the manufacturer's protocol. Incubation of cells with actinomycin D was used as a positive control for apoptosis. Fluorescence was detected by flow cytometry (FACS Calibur™; BD Biosciences, Palo Alto, CA, USA). Fluorescence parameters were gated using unstained cells. Data shown are expressed as percentages of Annexin V-positive cells for quantitation of apoptosis.[31,32]

Internalization assays

THP-1 cells (1×10^6/well) in serum-free RPMI-1640 were exposed to the Pep-1:GILZ-P complex at increasing molar

ratios of 0.1 to 50 and incubated at 37°C in a humidified 5% CO_2 chamber. Cells harvested at 15 minutes, 30 minutes, 1 hour, and 4 hours were lysed, and the cytoplasmic fraction was isolated using the nuclear cytoplasmic extraction kit following the manufacturer's protocol (Pierce Biotechnology, Rockford, IL, USA). An equal quantity of the cytoplasmic fraction (20 µL) in 100 µL of phosphate-buffered saline (PBS) was plated in 96-well high affinity enzyme-linked immunosorbent assay (ELISA) plates and probed for the presence of GILZ-P with 20 µM recombinant human p65 protein (rp65-DDK; OriGene Technologies, Inc., Rockville, MD, USA). Previously we observed that GILZ-P at 15 µM binds purified p65 protein with a dissociation constant of $1.12\pm0.25 \times 10^{-6}$ M.[27] Wells coated with Pep-1:GILZ-P at a specific molar ratio (0.1 to 50) constituted positive controls. The GILZ-P-bound p65 detected with anti-DDK monoclonal antibody was visualized by trinitrobenzene substrate and 2 N sulfuric acid. Absorbance at 450 nM was measured using an absorbance microplate reader (Model 680; Bio-Rad Laboratories, Hercules, CA, USA). Presence of GILZ-P was determined using the equation: % GILZ-P = $(OD_{treated} - OD_{cells\ only}/OD_{pos})*100$ (where OD represents optical density).

In separate experiments, THP-1 cells (1×10^6/well) cultured similarly in the presence of Pep-1:GILZ-P complex as above or with Pep-1:recombinant GILZ (rGILZ) (Abnova,Taipei City, Taiwan) at 20:1 molar ratio were permeabilized at the end of 24 hours. The presence of intracellular GILZ-P was determined by sequentially incubating the permeabilized cells with 20 µM rp65-DDK followed by phycoerythrin-conjugated anti-DDK monoclonal antibody at 4°C for 30 minutes. After washing briefly, the cells were fixed in 2% paraformaldehyde and analyzed immediately using a FACSCalibur flow cytometer. Mean fluorescence intensity was representative of the amount of GILZ-P-bound p65. Data are presented as the average of two independent experiments.

Cell proliferation

THP-1 macrophages (1×10^6/mL) were preincubated independently with 100 µL of 80 µM GILZ-P_c/Control-P_c/GILZ-P/Control-P/(2 µL) Pep-1 alone at 37°C in humidified 5% CO_2 for 30 minutes. The cells were then suspended in complete RPMI-1640 medium, seeded in 24-well plates in a total volume of 1 mL/well and cultured in the presence or absence of lipopolysaccharide (LPS) 2 µg/mL.[35] In some wells, the lipopolysaccharide-stimulated cells were treated with dexamethasone 0.3 mg/mL. At the end of 72 hours, 25 µL of MTT (3-[4,5-Dimethylthiazol-2-yl]-2,5-diphenyltetrazolium bromide) solution at 5.0 mg/mL was added to each well and incubated at 37°C for 3 hours. The plates were then centrifuged at 1,000 rpm in a clinical centrifuge for 5 minutes. The supernatants were removed and 150 µL of the MTT solvent (10% isopropanol and 50% sodium dodecyl sulfate) was added to each well and the plates were incubated at 37°C with mild shaking for 30 minutes. Optical density measurements were recorded at 540 nM absorbance using a Gensys 5 spectrophotometer (Thermo Fisher Scientific). The viability of THP-1 cells was indicated by the absorbance at 540 nM of the reduced formazan formed in living cells. The absorbance in all test samples was normalized to the cells cultured with medium-alone. All experiments were performed in triplicate and the data are presented as the mean ± standard deviation.

In independent experiments, THP-1 macrophages treated as above with 80 µM GILZ-P_c/Control-P_c/(2 µL) Pep-1 alone or dexamethasone were stimulated similarly with lipopolysaccharide 2 µg/mL or medium-alone. The supernatant was collected at the end of 24, 48, and 72 hours, and was stored at −80°C until further analysis.

ELISA for cytokines

Cytokines in the culture supernatant were measured by ELISA using Opt EIA kits for IFN-γ, IL-12, IL-6 (BD Biosciences) or Quantikine ELISA kits for TNF-α (R&D Systems, Minneapolis, IN, USA).[36] Briefly, 96-well enzyme immunoassay plates (Thermo Fisher Scientific) coated with the appropriate concentration of the primary antibody were applied 50 µL of culture supernatant in triplicates. The presence of cytokine was probed using the appropriate detection antibody and detected using the streptavidin enzyme conjugate followed by color development. The optical density of each well was determined using a microplate reader set to 450 nm. The concentration of cytokines was calculated in comparison with the standard series diluted in two-fold steps. Limits of detection were 31.2, 3.9, 3.9, and 7.8 pg/mL for IL-12, IFN-γ, IL-6, and TNF-α, respectively.

NFκB assay

THP-1 macrophages (1×10^6/mL) were preincubated with 100 µL of 80 µM GILZ-P_c/Control-P_c/(2 µL) Pep-1 alone at 37°C in humidified 5% CO_2 for 30 minutes. The cells were then suspended in serum-free RPMI-1640 medium, seeded in 24-well plates, and cultured in the presence or absence of LPS 2 µg/mL. In some wells, the LPS-stimulated cells were treated with dexamethasone 0.3 mg/mL. Nuclear extracts were prepared from cells harvested after 4 hours

of culture using the nuclear extraction kit following the recommended protocol (Active Motif). Activated NFκB in each sample was determined by oligonucleotide-based ELISA using the TransAM kit protocol (Active Motif). Five micrograms of nuclear extract was incubated in a 96-well plate coated with oligonucleotides containing the NFκB consensus nucleotide sequence (5′-GGGACTTTCC-3′). The activated NFκB bound to DNA was detected by the anti-p65 antibody followed by the horseradish peroxidase-conjugated secondary antibody and visualized using hydrogen peroxide/TMB (3,3′ 5,5′-tetramethylbenzidine) chromogenic substrate. The p65 binding was calculated as the ratio of absorbance of the LPS-stimulated cells to unstimulated cells for each test sample. Nuclear extracts of Raji cells provided in the kit were used as the positive control for nuclear p65. In separate experiments, to determine the dose response, the THP-1 macrophages preincubated with GILZ-P_c or Control-P_c at varying concentrations (10, 40, and 80 μM) were cultured similarly. The nuclear extracts harvested from cells at 4 hours were assessed for activated p65 as mentioned.

Glutamate production

THP-1 macrophages (0.5×10^6/well) pretreated with 80 μM GILZ-P_c/Control-P_c/(2 μL) Pep-1 alone were cultured in complete RPMI-1640 medium in the presence or absence of LPS 2 μg/mL as above. In some wells, the LPS-stimulated cells were treated with dexamethasone 0.3 mg/mL. The concentration of glutamate in the culture supernatant collected at the end of 24 hours was measured using a commercially available glutamate colorimetric assay following the manufacturer's protocol (BioVision Inc., Milpitas, CA, USA).[31,37] Briefly, glutamate standard (0, 2, 4, 6, 8, 10 nmol/well) and culture supernatant diluted 1:4 in the assay buffer provided in the kit was added to 96-well plates in triplicate. To each well was added a reaction mixture containing 0.8% glutamate developer and 0.2% glutamate enzyme mix in the assay buffer. The glutamate enzyme mix recognizes glutamate as a specific substrate leading to proportional yellow color development, and the amount of glutamate is measured by reading the absorbance at 450 nM in a microplate reader. Wells added assay buffer and developer in the absence of glutamate enzyme served as background controls. The net absorbance in supernatants of each sample calculated by subtracting the values of the background wells was used to determine the amount of glutamate using the standard curve. The glutamate concentration in each sample was calculated using the formula C = Sa/Sv nmol/μL, where Sa is the sample amount of known (in nmol) from the standard curve and Sv is the sample volume (μL) added into the wells. The low limit of detection was 2 nmol/μL. The experiment was repeated twice and the data presented represent the average of two experiments. To determine the dose response, in separate experiments the THP-1 macrophages preincubated with GILZ-P_c or Control-P_c at varying concentrations (10, 40, and 80 μM) were cultured similarly and supernatants collected at 24 hours were measured for glutamate secretion as mentioned.

Statistical analysis

Differences in the proliferation, cytokine secretion, glutamate production, and p65 activity between the untreated and treated (with GILZ-P_c/Control-P_c/dexamethasone/GILZ-P, Control-P/Pep-1 alone) macrophages were determined by pairwise comparison using the Student's *t*-test. A difference at $P \leq 0.05$ was considered to be statistically significant.

Results and discussion

Rationale and design of GILZ-P

The carboxy terminus of GILZ (GILZ-COOH) spans 40 residues (98–137), with eight glutamic acid residues, eight prolines, and five "PXXP" motifs[14,21] (Figure 1A). The primary sequence of GILZ is highly homologous to that of porcine δ sleeping-inducing peptide (DSIP). In models of GILZ generated using the solution structure of DSIP (PDB:1 DIP) as a template, secondary structure assignment by PROSS showed that the Pro123 of human GILZ exhibits φ and ϕ angles of −64.5° and 149.8°, respectively, adopting a helical poly-l-proline type II (PPII) conformation[27,38,39] (Figure 1B). The presence of multiple glutamic acid residues in the region increases the net charge, further promoting the extended PPII conformation by electrostatic repulsion.[40] Replacement of both glutamic acid and the proline residues in the proline-rich region by alanine abrogated the ability of GILZ to inhibit NFκB, potentially due to an induced bend that disrupts the extended PPII conformation[21,22] (Figure 1C). Binding studies suggested that the GILZ protein interacts with the transactivation domain at the carboxy terminus of p65.[27] Similar to the frequently observed features in structural complexes with fast binding kinetics, the C-H-π interaction between the imino ring of the critical prolines of GILZ and the aromatic ring of the conserved F534 and F542 in the p65 transactivation domain could contribute to the binding energy of the GILZ:p65 complex.[41–43] The planar structure of the aromatic side chains are complementary to the ridges and grooves presented on the PPII helix.[41,43] Taken together,

these observations implicate a short proline-rich motif at the GILZ-COOH as critical for interacting with and inhibiting p65 transactivation.

Considerable success has been achieved in adopting the results from mutagenesis and structural studies to design small molecule antagonists of protein-protein interactions.[44,45] This approach relies on the premise that the key residues of the binding epitope, in particular the side chain functional groups responsible for the binding affinity between two proteins may be transferred to a much smaller molecule with contributions to the binding largely intact.[44,46] The approach is particularly effective for proline-rich motifs that preferentially adopt a helical PPII conformation, since absence of the backbone hydrogen donor on proline allows the free carbonyls to participate in intermolecular hydrogen bonds. In contrast with the enthalpy-induced associations, such as the lock and key model, PPII helices are entropy-driven and behave as "adaptable gloves" in order to obtain the correct recognition.[47] Further, the side chain and the backbone carbonyls that point outwards at regular intervals can be easily "read" by the interacting protein, making the PPII helix an excellent recognition motif[40] and potential therapeutic lead. We hypothesized that a peptide derived from the proline-rich carboxy terminus of GILZ (ie, GILZ-P) would adopt a helical PPII conformation and inhibit p65 transactivation.[47] To mimic the end groups of the p65 binding domain of GILZ and to stabilize the secondary structure, GILZ-P was synthesized as an amide with acetylation of the amino terminus.[28]

GILZ-P adopts a helical PPII conformation

The best way to unambiguously reveal the PPII structure in solution is to use spectroscopies based on optical activity, such as CD. As seen in Figure 2A, the CD spectrum of GILZ-P presented a strong negative band ($\theta = -20.03\times10^3$ deg·cm^2/dmol) at 199 nm and a weak positive band ($\theta = 1.12\times10^3$ deg cm^2/dmol) at 238 nm, consistent with the spectrum of polypeptides that prefer a helical PPII structure.[8,15] An increase in temperature to 90°C or spectral analysis of GILZ-P in 5 M $CaCl_2$ resulted in a dramatic decrease in the intensity of the mean residue ellipticity minimum ($\theta = -8.84\times10^3$deg·cm^2/dmol at 205 nM and $\theta = -11.37\times0^3$deg·cm^2/dmol at 204 nM, respectively) due to transition from the PPII helix to random coil conformation[13] (Figure 2A). The CD spectrum of Control-P1 and Control-P2 at 194 nm showed a weak minimum of $\theta = 4.5\times10^1$ deg·cm^2/dmol and $\theta = -3.5\times10^1$ deg·cm^2/dmol, respectively (Figure 2B). Control-P1 was used in further cellular experiments.

Effects of GILZ-P on cell viability and apoptosis

GILZ-P is developed as a potential NFκB inhibitory agent. As a first step to investigate the possibility of using GILZ-P in humans, we assessed the effect of GILZ-P on the viability of human macrophage-like THP-1 cells by trypan blue exclusion using an automated cell counter.[34] THP-1 cells were treated with increasing concentrations of GILZ-P_c (10–640 μM). The range of concentration is equivalent to 0.028–1.8 mg/mL and represents the dose range commonly used for peptide therapeutics.[48–50] The viability of cells was assessed at 1, 4, 8, 12, 24, and 48 hours following exposure to GILZ-P_c. Cells cultured in medium-alone maintained viability of 70%–100% at all time points (Figure 3A). Although the viability of THP-1 cells decreased with increasing concentrations of GILZ-P_c, more than 40% of cells remained viable, even in cultures treated with the highest concentration of

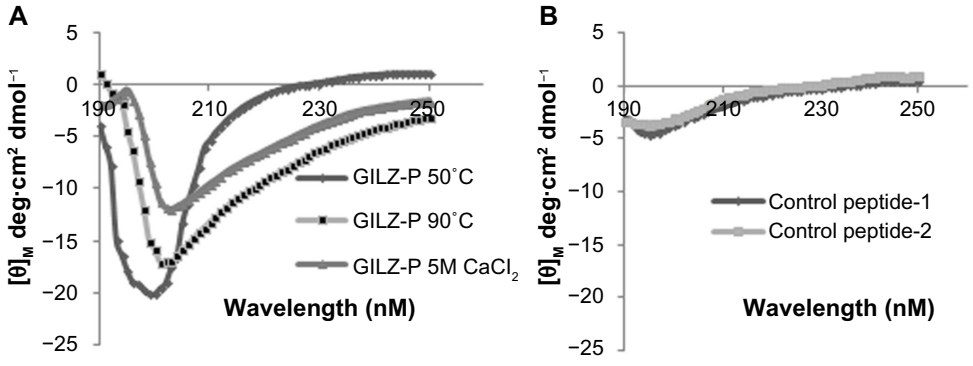

Figure 2 Secondary structure of GILZ-P by circular dichroism.
Notes: Circular dichroism spectra of (**A**) GILZ-P and (**B**) control peptide 1 and 2 (100 μM in water) at 50°C in 1 mM sodium citrate, 1 mM sodium borate, 1 mM sodium phosphate buffer, and 15 mM NaCl with the pH adjusted to 7.0 or in 5 M $CaCl_2$. 190 and 240 represent the range of wavelength.
Abbreviations: GILZ, glucocorticoid-induced leucine zipper; GILZ-P, synthetic peptide derived from the proline-rich region of GILZ.

GILZ-P_c at 640 μM (Figure 3B). The mean percent viability of cells exposed to 640 μM GILZ-P_c at 1 hour and 48 hours was 72%±4.5% and 45%±5.5%, respectively.

We next investigated the cellular toxicity of GILZ-P by staining for the apoptosis-specific and necrosis-specific markers, Annexin V and propidium iodide, respectively. Flow cytometric analysis showed that the mean percent apoptosis of THP-1 cells cultured in medium-alone and harvested at 4, 8, and 24 hours was 0.32±0.7, 0.53±0.7, and 1.003±0.22, respectively (data not shown). Representative histograms of percent apoptosis in THP-1 cultures exposed to 0, 40, or 80 μM of GILZ-P_c at 4, 8, and 24 hours are shown in Figure 3D–F. A dramatic increase was observed in the mean percent apoptosis of THP-1 cells treated with 80 μM (3.48±0.4%) GILZ-P_c as compared with cells exposed to 40 μM GILZ-P_c (1.03±0.24%) at the 4-hour time

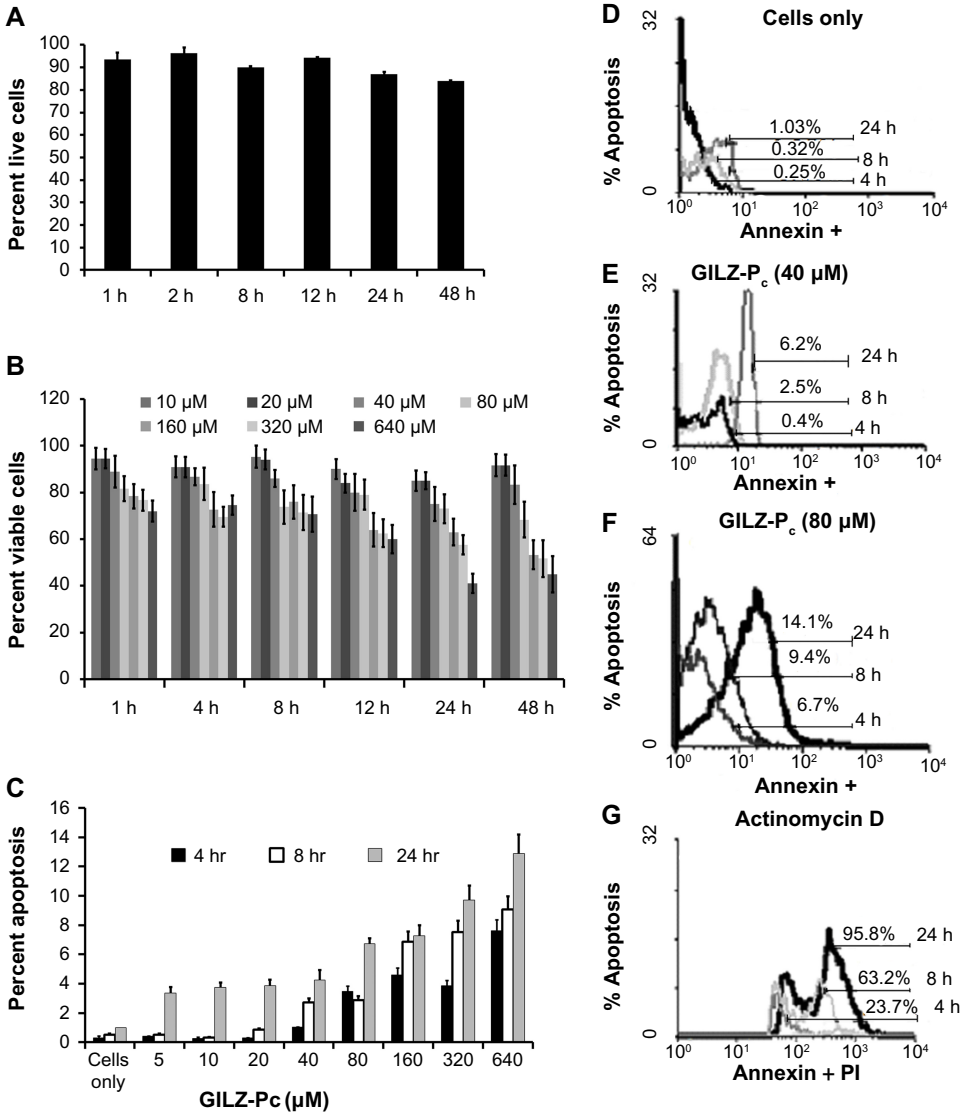

Figure 3 Effect of GILZ-P on viability of THP-1 monocytes.

Notes: THP-1 cells were incubated with increasing concentrations of GILZ-P_c from 10 μM to 640 μM at 37°C for increasing time periods from 1 hour to 48 hours. The control consisted of cells incubated in medium-alone. At indicated time points, the percentage of live cells was determined by trypan blue exclusion. (**A**) Shows percentage viability in control cells cultured in medium at indicated time points. (**B**) Represents the percentage of live cells treated with the indicated concentration of GILZ-P_c at specified times. Data are normalized with respect to the cells cultured in medium-alone at each time point and represent the mean ± standard deviation of three independent experiments. (**C**) GILZ-P-treated macrophages stimulated with LPS and treated similarly were stained with Annexin V (apoptosis marker) and propidium iodide (necrosis marker) and subjected to fluorescence-activated cell sorting analysis to determine apoptosis. The mean percentage of Annexin V-positive THP-1 cells treated with GILZ-P_c at indicated concentrations and analyzed at indicated time points is shown. Data represent the mean ± standard deviation of three independent experiments. Representative histogram of the percentage of apoptosis in THP-1 cultures exposed to (**D**) 0, (**E**) 40 μM, or (**F**) 80 μM of GILZ-P_c at indicated time point is shown. (**G**) Representative histogram of dual positive (Annexin V and propidium iodide) THP-1 cells treated with actinomycin D as the positive control.

Abbreviations: GILZ, glucocorticoid-induced leucine zipper; GILZ-P, synthetic peptide derived from the proline-rich region of GILZ; GILZ-P_c, noncovalent complex of Pep-1 with GILZ-P; LPS, lipopolysaccharide; h, hours.

point (Figure 3C). The mean percent apoptosis of THP-1 cells exposed to GILZ-P_c at the highest concentration of 640 μM at 4, 8, and 24 hours was 7.62±0.3%, 9.06±1.9% and 12.88±2.9%, respectively (Figure 3C). The mean percent dual positive THP-1 cells (apoptotic and necrotic) exposed to 80 μM or 640 μM of GILZ-P_c at 24 hours was 28.9±1.01% and 60.3±3.2%, respectively. The mean percent dual positive THP-1 cells treated with actinomycin D and harvested at 4, 8, and 24 hours was 26.9±7.5%, 59.1±9.2%, and 98.4±2.1%, respectively. A representative histogram of dual positive THP-1 cells treated with actinomycin D is shown in Figure 3G. Collectively, these observations suggest that GILZ-P is largely nontoxic.

GILZ-P prevents LPS-induced proliferation and cytokine secretion

GILZ-P acts by binding p65 in the cytoplasm and should be delivered into the cell to be effective as a therapeutic agent.[28] Cytoplasmic fractions of THP-1 cells exposed to increasing concentrations of Pep-1:GILZ-P complex were assessed for binding purified p65 as a measure of intracellular presence of GILZ-P by modified ELISA. The highest intracellular presence of GILZ-P was observed in cells exposed to a 10:1 molar ratio of Pep-1:GILZ-P (Figure 4A). In addition, a dose response of intracellular concentration of GILZ-P was observed during early time points. In separate experiments, THP-1 cells exposed to increasing molar ratios of Pep:1-GILZ-P complex were permeabilized at the end of 24 hours. The permeabilized cells were probed with rp65-DDK as an indirect measure of intracellular GILZ-P. Flow cytometric analysis of permeabilized THP-1 cells showed that the maximum internalization of the peptide was observed in cells exposed to GILZ-P:Pep-1 at a 1:10 molar ratio (Figure 4B). Interestingly, with increasing concentrations of Pep-1, the internalization efficiency was reduced (Figure 4A and B). Similar observations for cargo delivery by Pep-1 have been reported previously.[51]

To determine the inhibitory potential, we next assessed the functional efficacy of GILZ-P_c in PMA-differentiated THP-1 macrophages. The membrane integrity and proliferation of THP-1 macrophages stimulated with LPS and treated with dexamethasone/80 μM GILZ-P_c/Control-P_c, GILZ-P/Control-P/(0.2 μL) Pep-1 alone for 72 hours was determined by MTT colorimetric assay. The viability of THP-1 cells (as indicated by absorbance at 540 nM) was significantly higher in cultures treated with dexamethasone (228.5±23.6)/GILZ-P_c (251±14.5) than in untreated cultures (168.3±19.6) or Control-P_c-treated cultures (175.6±9.1, Figure 5A). No significant difference was observed in viability of cells stimulated in the presence of GILZ-P (165.8±10)/Control-P (149.6±13.8)/Pep-1 alone (133.3±0.3) as compared with untreated cells (168.3±19.6, Figure 5A).

We then investigated whether the reduced proliferative index mediated by GILZ-P_c was reflected by cytokine secretion in LPS-stimulated THP-1 macrophages. Measurement of cytokines by ELISA suggested that at the end of 24 hours, macrophages stimulated with LPS and treated with GILZ-P_c 80 μM or dexamethasone 0.3 mg/mL

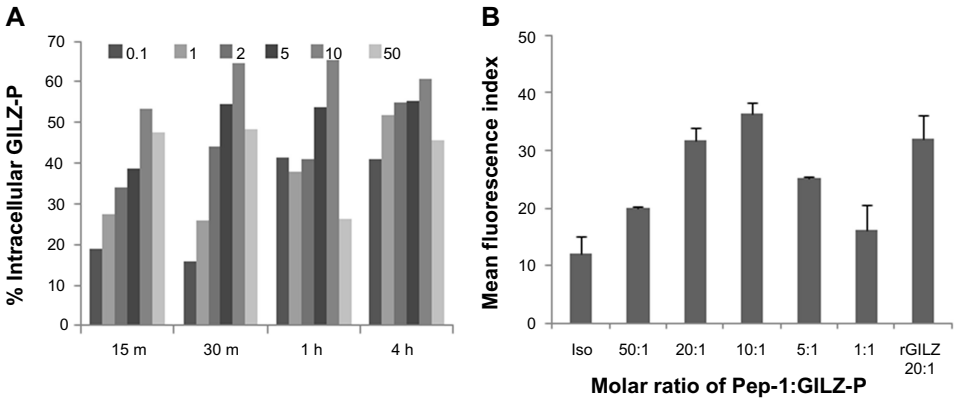

Figure 4 Intracellular delivery of GILZ-P.

Notes: THP-1 macrophages (1×10^6/mL) were cultured in serum-free RPMI-1640 medium with an increasing molar ratio of Pep-1:GILZ-P complex at 37°C in humidified 5% CO_2. The GILZ-P:rp65-DDK complex was detected as a measure of intracellular GILZ-P. (**A**) The percentage of GILZ-P in the cytoplasmic fraction of cells harvested at the indicated time points by modified enzyme linked immunosorbent assay (ELISA). In separate experiments (**B**), THP-1 cells cultured similarly were harvested at the end of 24 hours. In permeabilized cells, intracellular GILZ-P was probed for binding of recombinant human p65 protein and was assessed by flow cytometry. (**B**) Mean fluorescence intensity, representative of the amount of GILZ-P-bound p65, is shown. The data represent the mean of two independent experiments. *$P<0.05$.

Abbreviations: GILZ, glucocorticoid-induced leucine zipper; GILZ-P, synthetic peptide derived from the proline-rich region of GILZ; h, hours; Iso, isotype; m, minutes; rGILZ, recombinant GILZ; RPMI, Roswell Park Memorial Institute.

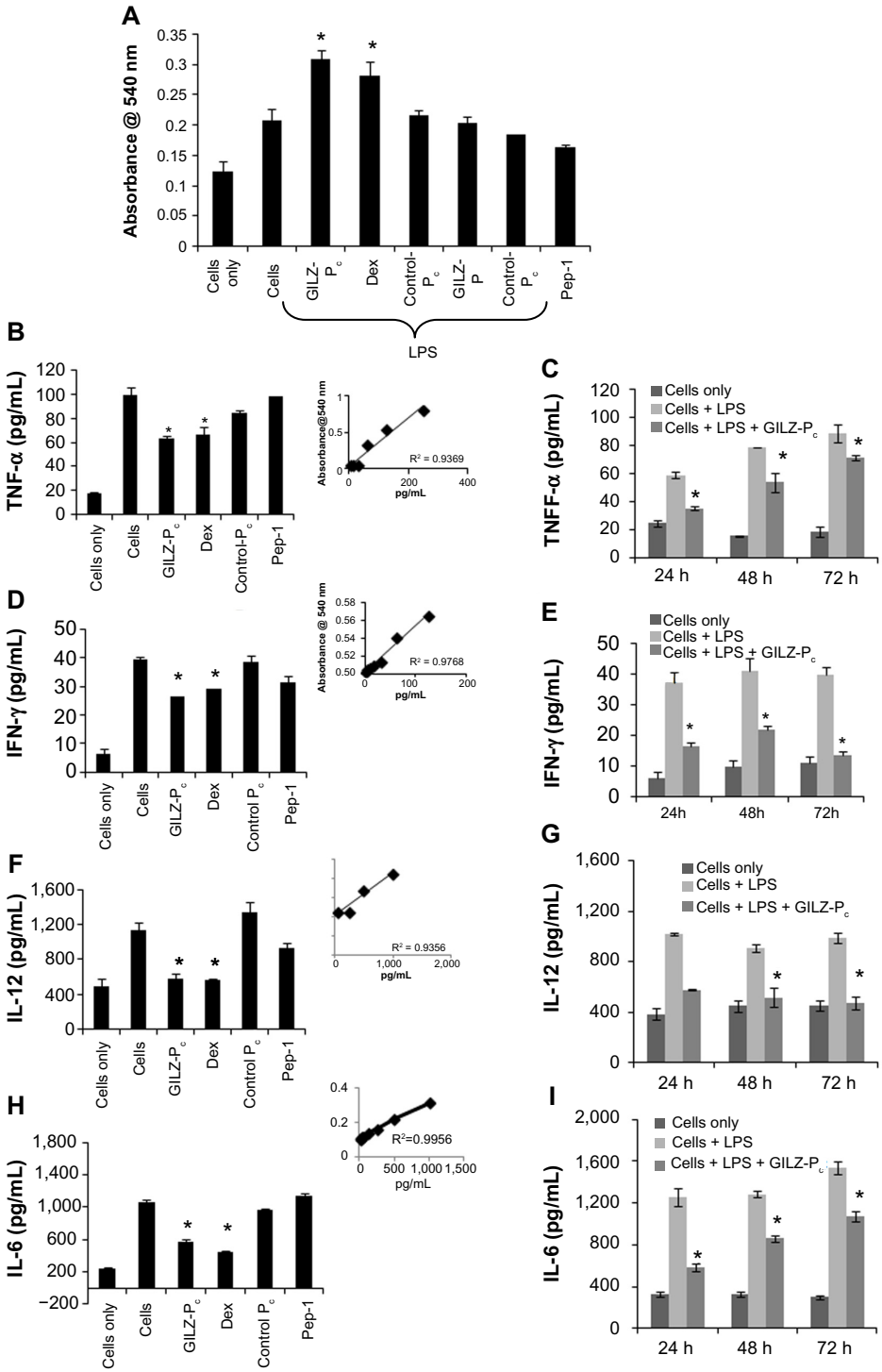

Figure 5 Effect of GILZ-P on proliferation and cytokine responses.

Notes: THP-1 cells (1×10^6/mL) in 100 μL of serum-free RPMI-1640 medium were preincubated in 100 μL of 80 μM GILZ-P_c, Control-P_c, GILZ-P, Control-P, or (2 μL) Pep-1 at 37°C in humidified 5% CO_2 for 30 minutes. In some cultures, THP-1 cells were treated with dexamethasone 0.3 mg/mL. The cells were then suspended in complete RPMI-1640 medium and cultured in the presence or absence of LPS 2 μg/mL for 72 hours. Cell viability was determined by the colorimetric MTT assay (**A**). Values are normalized for the cells cultured in medium-alone. The data represent the mean ± standard deviation of three independent experiments. *$P<0.05$. In separate experiments, supernatants collected at 24 hours from THP-1 macrophages cultured similarly were assessed for specific cytokines (**B**, **D**, **F** and **H**) by ELISA. To determine kinetics, the supernatant from separate THP-1 cultured cells was similarly harvested at the end of 24, 48, and 72 hours and the indicated cytokines were measured. (**C**, **E**, **G** and **I**). The cytokine concentrations in the samples were calculated in comparison with standard series (insets). The data represent the mean of three independent experiments. *$P<0.05$.

Abbreviations: ELISA, enzyme-linked immunosorbent assay; GILZ, glucocorticoid-induced leucine zipper; GILZ-P, synthetic peptide derived from the proline-rich region of GILZ; LPS, lipopolysaccharide; GILZ-P_c, noncovalent complex of Pep-1 with GILZ-P; MTT, 3-(4,5-dimethyl-thiazol-2-yl)-2,5 diphenyl tetrazolium bromide; TNF-a, tumor necrosis factor-a; IFN-γ, interferon gamma; Dex, dexamethasone; RPMI, Roswell Park Memorial Institute.

secreted significantly less TNF-α, IL-12, IFN-γ, and IL-6 as compared with the untreated or Control-P_c-treated cells (Figure 5B, D, F, and H). Time course analysis suggested that the reduction in TNF-α and IL-6 was more pronounced at 24 hours (Figure 5C and I) and that IFN-γ production was most significant in 72-hour cultures of GILZ-P_c-treated THP-1 macrophages (Figure 5E). The concentration of IL-12 was significantly lower in LPS-stimulated GILZ-P_c-treated cells at all time points measured as compared with the untreated THP-1 cells (Figure 5G). Taken together, these observations suggest that GILZ-P at a concentration of 80 μM inhibits proliferation and proinflammatory cytokine secretion by LPS-stimulated mature macrophages.

GILZ-P treatment inhibits activated p65

LPS stimulation has previously been shown to enhance expression of activated NFκB in naïve THP-1 cells as well as in PMA-differentiated THP-1 macrophages.[33] We measured nuclear p65 using activated NFκB-specific ELISA and report the p65 binding activity as the ratio of absorbance in nuclear extracts from LPS-stimulated THP-1 macrophages to that in unstimulated cells. LPS-stimulated THP-1 macrophages treated with dexamethasone/GILZ-P_c exhibited reduced nuclear p65 as compared with untreated cells (Figure 6A). A dose-dependent reducing trend of nuclear p65 was observed in LPS-stimulated GILZ-P_c-treated THP-1 macrophages (Figure 6B). Treatment with Control-P_c, GILZ-P, or Pep-1 alone was not associated with a significant difference in nuclear p65 as compared with the untreated cells (Figure 6A and B). Collectively, these observations suggest that, much like glucocorticoids and other synthetic agents, such as aspirin and nanocurcumin,[52–56] GILZ-P treatment also potentially suppresses cytokine responses by inhibiting NFκB activity.

GILZ-P suppresses glutamate release by LPS-stimulated mature THP-1 cells

In addition to the measurement of the cytokines and NFκB activation, assessment of other biologically active molecules integrally involved in the pathological process, such as glutamate in neuroinflammatory diseases, is often assessed as outcomes in early stages of drug discovery.[30,57] We investigated whether treatment with GILZ-P could modulate glutamate secretion in LPS-stimulated THP-1 cells secondary to the observed NFκB blockade. A measurable amount of glutamate (395.5±22.4 μM) was detected in the supernatant of unstimulated THP-1 cells (Figure 7A). LPS stimulation upregulated release of glutamate by THP-1 macrophages (886.6±20.9 μM) and treatment with GILZ-P_c (595±22 μM) or dexamethasone (416.37±21.7 μM) significantly suppressed glutamate production (Figure 7A). The reduction in glutamate release was observed at all concentrations of GILZ-P_c assessed (Figure 7B). No difference was observed in glutamate production in THP-1 cultures stimulated in the presence of Control-P_c (792.3±42.6 μM) or Pep-1 alone

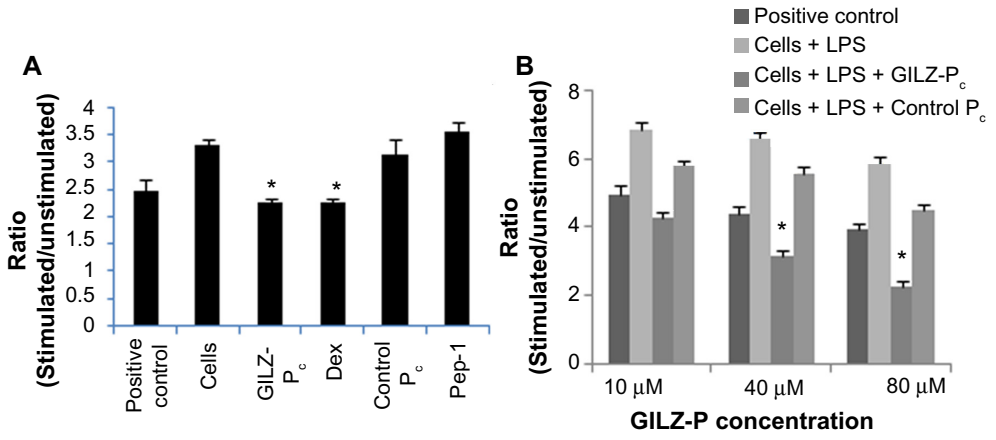

Figure 6 Effect of GILZ-P on NFκB activation in macrophages.

Notes: (**A**) THP-1 macrophages (1 × 10^6/mL) were preincubated with 80 μM GILZ-P_c, Control-P_c, or (2 μL) Pep-1 alone at 37°C in humidified 5% CO_2 for 30 minutes. The cells were then cultured in serum-free medium in the presence or absence of LPS (2 μg/mL). Some cells were stimulated in the presence of dexamethasone 0.3 mg/mL. Nuclear extracts obtained from cells harvested at the end of 4 hours were tested for binding of the activated p65 NFκB subunit to an NFκB consensus sequence using the TransAM NFκB ELISA kit. (**A**) p65 DNA binding activity was calculated as the ratio of absorbance from LPS-stimulated cells to that of unstimulated cells. (**B**) To determine the dose effect, THP-1 cells preincubated with increasing concentrations (10, 40, and 80 μM) of GILZ-P_c or Control-P_c were cultured similarly in separate experiments and the nuclear extracts assessed for activated p65. The mean absorbance of cells cultured in medium-alone at 450 nM varied between 0.112 and 0.245. Values are the mean ± standard deviation of three experiments performed in duplicate. *$P<0.05$.

Abbreviations: ELISA, enzyme-linked immunosorbent assay; GILZ, glucocorticoid-induced leucine zipper; GILZ-P, synthetic peptide derived from the proline-rich region of GILZ; GILZ-P_c, noncovalent complex of Pep-1 with GILZ-P; LPS, Lipopolysaccharide; Dex, dexamethasone.

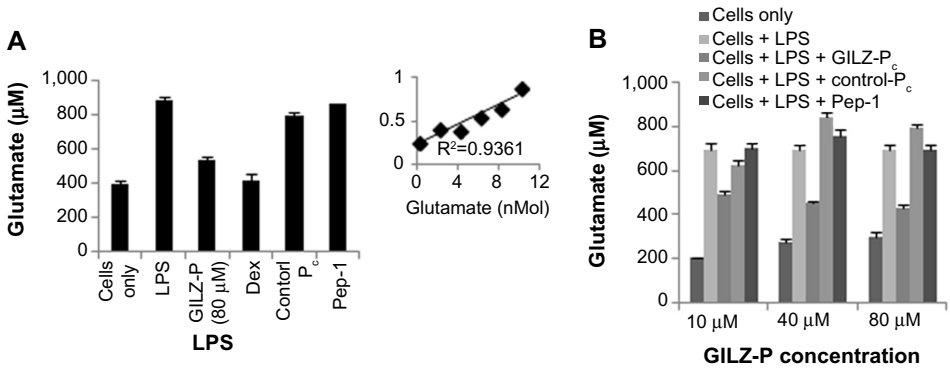

Figure 7 Effects of GILZ-P on glutamate concentration in cultures of human macrophages.

Notes: THP-1 macrophages (1×10^6/mL) were preincubated with 80 μM GILZ-P_c, Control-P_c, or (2 μL) Pep-1 alone at 37°C in humidified 5% CO_2 for 30 minutes. The cells were then cultured in complete RPMI-1640 medium in the presence or absence of LPS (2 μg/mL) for 24 hours. In some wells, the LPS-stimulated cells were treated with dexamethasone 0.3 mg/mL. (**A**) Glutamate concentrations in the supernatants measured using a specific colorimetric assay. Concentrations of glutamate in the samples were calculated in comparison with standard series (inset). (**B**) To determine the dose effect, THP-1 cells preincubated with increasing concentrations (10, 40, and 80 μM) of GILZ-P_c or Control-P_c were cultured similarly in separate experiments and the supernatants were assessed for glutamate release. Samples were analyzed in triplicate and the data represent the mean of three independent experiments. *$P<0.05$ as compared with cells stimulated with LPS.

Abbreviations: GILZ, glucocorticoid-induced leucine zipper; GILZ-P, synthetic peptide derived from the proline-rich region of GILZ; GILZ-P_c, noncovalent complex of Pep-1 with GILZ-P; LPS, lipopolysaccharide; Dex, dexamethasone; RPMI, Roswell Park Memorial Institute.

(700.16±7.2 μM) as compared with that in untreated cells (605.1±20.2 μM, Figure 7B). Thus, much like prednisolone,[30] GILZ-P also inhibits glutamate secretion via activated macrophages, suggesting a potential neuroprotective effect for the latter.

Conclusion and future directions

Proline-rich motifs participating in intermolecular interactions constitute excellent drug targets for development of competitive inhibitors. For example, a peptide derived from the proline-rich region of the Wiskott-Aldrich syndrome protein (WASP)-interacting protein ameliorated the defects in reorganization of the actin cytoskeleton.[26] Previously, we have shown that peptide mimics of the polyproline epitope of the CD28 receptor suppressed the immune response by interfering with CD28: ligand interactions.[28,58] Here we demonstrate that a peptide derived from the p65 binding proline-rich motif of the GILZ protein adopts a helical PPII conformation, effectively suppresses NFκB activation, and suppresses neurotoxic glutamate in differentiated human macrophage-like cells used as a model for microglial cells. Intraperitoneal administration of GILZ-P at 500 μg ameliorated disease in a mouse model of multiple sclerosis.[27] Further, treatment with GILZ-P was not associated with signs of osteoporosis in mice, indicating that the peptide agent potentially bypasses the adverse effects of glucocorticoids.[59] Collectively, these observations strongly support the therapeutic potential of GILZ-P in chronic inflammatory conditions, including neuroinflammatory pathologies transitioning to neurodegenerative diseases.[60] Further structural and biophysical characterization of the GILZ:p65 interaction will assist in the design of functionally efficient small-molecule GILZ-P analogs.

Acknowledgments

We sincerely appreciate the grant supports from the Indiana CTSI to MS and DKL. This work was also partly supported by grants from National Institutes of Health (NIA-R01 and -R21) and Alzheimer's Association (IIRG) to DKL. We sincerely appreciate assistance from Mr. Nipun Chopra in some of the procedures.

Disclosure

DKL: Scientific advisory board – QR Pharma, Yuma Therapeutics, Entia Biosciences; International advisory board – Drug Discovery and Therapy World Congress; stock options, QR Pharma; patent involving AIT-082, memantine and pending on acamprosate; Editor in Chief, Current Alzheimer Research; research grant support from Baxter Healthcare. MS: cofounder, Provaidya LLC., Indianapolis. CB reports no conflicts of interest in this work.

These disclosures and the funding sources noted in the Acknowledgment section had no role in study design, in the collection, analysis, and interpretation of data, in the writing of the report, or in the decision to submit the article for publication.

References

1. Bacher S, Schmitz ML. The NF-kappaB pathway as a potential target for autoimmune disease therapy. *Curr Pharm Des*. 2004;10(23):2827–2837.

2. Grilli M, Memo M. Nuclear factor-kappaB/Rel proteins: a point of convergence of signalling pathways relevant in neuronal function and dysfunction. *Biochem Pharmacol*. 1999;57(1):1–7.
3. Roman-Blas JA, Jimenez SA. NF-kappaB as a potential therapeutic target in osteoarthritis and rheumatoid arthritis. *Osteoarthritis Cartilage*. 2006;14(9):839–848.
4. Yamamoto Y, Gaynor RB. Therapeutic potential of inhibition of the NF-kappaB pathway in the treatment of inflammation and cancer. *J Clin Invest*. 2001;107(2):135–142.
5. Yan J, Greer JM. NF-kappa B, a potential therapeutic target for the treatment of multiple sclerosis. *CNS Neurol Disord Drug Targets*. 2008;7(6):536–557.
6. Brown GC, Neher JJ. Inflammatory neurodegeneration and mechanisms of microglial killing of neurons. *Mol Neurobiol*. 2010;41(2–3):242–247.
7. Tak PP, Firestein GS. NF-kappaB: a key role in inflammatory diseases. *J Clin Invest*. 2001;107(1):7–11.
8. Pande V, Ramos MJ. NF-kappaB in human disease: current inhibitors and prospects for de novo structure based design of inhibitors. *Curr Med Chem*. 2005;12(3):357–374.
9. Lleo A, Galea E, Sastre M. Molecular targets of non-steroidal anti-inflammatory drugs in neurodegenerative diseases. *Cell Mol Life Sci*. 2007;64(11):1403–1418.
10. Rao NA, McCalman MT, Moulos P, et al. Coactivation of GR and NFKB alters the repertoire of their binding sites and target genes. *Genome Res*. 2011;21(9):1404–1416.
11. Potter C, Cordell HJ, Barton A, et al. Association between anti-tumour necrosis factor treatment response and genetic variants within the TLR and NF{kappa}B signalling pathways. *Ann Rheum Dis*. 2010;69(7):1315–1320.
12. Fraser JH, Rincon M, McCoy KD, Le Gros G. CTLA4 ligation attenuates AP-1, NFAT and NF-kappaB activity in activated T cells. *Eur J Immunol*. 1999;29(3):838–844.
13. Fan H, Morand EF. Targeting the side effects of steroid therapy in autoimmune diseases: the role of GILZ. *Discov Med*. 2012;13(69):123–133.
14. Cannarile L, Zollo O, D'Adamio F, et al. Cloning, chromosomal assignment and tissue distribution of human GILZ, a glucocorticoid hormone-induced gene. *Cell Death Differ*. 2001;8(2):201–203.
15. D'Adamio F, Zollo O, Moraca R, et al. A new dexamethasone-induced gene of the leucine zipper family protects T lymphocytes from TCR/CD3-activated cell death. *Immunity*. 1997;7(6):803–812.
16. Ayroldi E, Zollo O, Bastianelli A, et al. GILZ mediates the antiproliferative activity of glucocorticoids by negative regulation of Ras signaling. *J Clin Invest*. 2007;117(6):1605–1615.
17. Berrebi D, Bruscoli S, Cohen N, et al. Synthesis of glucocorticoid-induced leucine zipper (GILZ) by macrophages: an anti-inflammatory and immunosuppressive mechanism shared by glucocorticoids and IL-10. *Blood*. 2003;101(2):729–738.
18. Cannarile L, Cuzzocrea S, Santucci L, et al. Glucocorticoid-induced leucine zipper is protective in Th1-mediated models of colitis. *Gastroenterology*. 2009;136(2):530–541.
19. Cannarile L, Fallarino F, Agostini M, et al. Increased GILZ expression in transgenic mice up-regulates Th-2 lymphokines. *Blood*. 2006;107(3):1039–1047.
20. Di Marco B, Massetti M, Bruscoli S, et al. Glucocorticoid-induced leucine zipper (GILZ)/NF-kappaB interaction: role of GILZ homodimerization and C-terminal domain. *Nucleic Acids Res*. 2007;35(2):517–528.
21. Ayroldi E, Riccardi C. Glucocorticoid-induced leucine zipper (GILZ): a new important mediator of glucocorticoid action. *FASEB J*. 2009;23(11):3649–3658.
22. Riccardi C. GILZ (glucocorticoid-induced leucine zipper), a mediator of the anti-inflammatory and immunosuppressive activity of glucocorticoids. *Ann Ig*. 2010;22(1 Suppl 1):53–59.
23. Ayroldi E, Migliorati G, Bruscoli S, et al. Modulation of T-cell activation by the glucocorticoid-induced leucine zipper factor via inhibition of nuclear factor kappaB. *Blood*. 2001;98(3):743–753.
24. Ball LJ, Kuhne R, Schneider-Mergener J, Oschkinat H. Recognition of proline-rich motifs by protein-protein-interaction domains. *Angew Chem Int Ed Engl*. 2005;44(19):2852–2869.
25. Ravi Chandra B, Gowthaman R, Raj Akhouri R, Gupta D, Sharma A. Distribution of proline-rich (PxxP) motifs in distinct proteomes: functional and therapeutic implications for malaria and tuberculosis. *Protein Eng Des Sel*. 2004;17(2):175–182.
26. Srinivasan M, Dunker AK. Proline rich motifs as drug targets in immune mediated disorders. *Int J Pept*. 2012;2012:634769.
27. Srinivasan M, Janardhanam S. Novel p65 binding glucocorticoid-induced leucine zipper peptide suppresses experimental autoimmune encephalomyelitis. *J Biol Chem*. 2011;286(52):44799–44810.
28. Srinivasan M, Wardrop RM, Gienapp IE, Stuckman SS, Whitacre CC, Kaumaya PT. A retro-inverso peptide mimic of CD28 encompassing the MYPPPY motif adopts a polyproline type II helix and inhibits encephalitogenic T cells in vitro. *J Immunol*. 2001;167(1):578–585.
29. Wang MH, Frishman LJ, Otteson DC. Intracellular delivery of proteins into mouse Muller glia cells in vitro and in vivo using Pep-1 transfection reagent. *J Neurosci Methods*. 2009;177(2):403–419.
30. Klegeris A, Walker DG, McGeer PL. Regulation of glutamate in cultures of human monocytic THP-1 and astrocytoma U-373 MG cells. *J Neuroimmunol*. 1997;78(1–2):152–161.
31. Lee M, Suk K, Kang Y, McGeer E, McGeer PL. Neurotoxic factors released by stimulated human monocytes and THP-1 cells. *Brain Res*. 2011;1400:99–111.
32. Harrison LM, Cherla RP, van den Hoogen C, et al. Comparative evaluation of apoptosis induced by Shiga toxin 1 and/or lipopolysaccharides in human monocytic and macrophage-like cells. *Microb Pathog*. 2005;38(2–3):63–76.
33. Sharif O, Bolshakov VN, Raines S, Newham P, Perkins ND. Transcriptional profiling of the LPS induced NF-kappaB response in macrophages. *BMC Immunol*. 2007;8:1.
34. Mertlikova-Kaiserova H, Votruba I, Matousova M, Holy A, Hajek M. Role of caspases and CD95/Fas in the apoptotic effects of a nucleotide analog PMEG in CCRF-CEM cells. *Anticancer Res*. 2010;30(7):2791–2798.
35. Cen O, Gorska MM, Stafford SJ, Sur S, Alam R. Identification of UNC119 as a novel activator of SRC-type tyrosine kinases. *J Biol Chem*. 2003;278(10):8837–8845.
36. Srinivasan M, Gienapp IE, Stuckman SS, et al. Suppression of experimental autoimmune encephalomyelitis using peptide mimics of CD28. *J Immunol*. 2002;169(4):2180–2188.
37. Klegeris A, Walker DG, McGeer PL. Toxicity of human THP-1 monocytic cells towards neuron-like cells is reduced by non-steroidal anti-inflammatory drugs (NSAIDs). *Neuropharmacology*. 1999;38(7):1017–1025.
38. Srinivasan M, Janardhanam S. Novel p65 binding glucocorticoid-induced leucine zipper peptide suppresses experimental autoimmune encephalomyelitis. *J Biol Chem*. 2011;286(52):44799–44810.
39. Srinivasan R, Rose GD. A physical basis for protein secondary structure. *Proc Natl Acad Sci U S A*. 1999;96(25):14258–14263.
40. Cubellis MV, Caillez F, Blundell TL, Lovell SC. Properties of polyproline II, a secondary structure element implicated in protein-protein interactions. *Proteins*. 2005;58(4):880–892.
41. Freund C, Schmalz HG, Sticht J, Kühne R. Proline-rich sequence recognition domain (PRD): ligands, function and inhibition. In: Klussmann E, Scott J, editors. *Protein-Protein Interactions as New Drug Targets*. Heidelberg, Berlin, Germany: Springer-Verlag; 2008.
42. Gu W, Helms V. Dynamical binding of proline-rich peptides to their recognition domains. *Biochim Biophys Acta*. 2005;1754(1–2):232–238.
43. Zarrinpar A, Bhattacharyya RP, Lim WA. The structure and function of proline recognition domains. *Sci STKE*. 2003;2003(179):RE8.

44. Eguchi M, Kahn M. Design, synthesis, and application of peptide secondary structure mimetics. *Mini Rev Med Chem*. 2002; 2(5):447–462.
45. Srinivasan M, Roeske RW. Immunomodulatory peptides from IgSF proteins: a review. *Curr Protein Pept Sci*. 2005;6(2):185–196.
46. Cochran AG. Antagonists of protein-protein interactions. *Chem Biol*. 2000;7(4):R85–R94.
47. Unal EB, Gursoy A, Erman B. Conformational energies and entropies of peptides, and the peptide-protein binding problem. *Phys Biol*. 2009;6(3):036014.
48. Groner B, editor. *Peptides as Drugs: Discovery and Development*. Weinheim, Germany: Wiley-VCH Verlag GmbH & Co KGaA; 2009.
49. Guan QH, Pei DS, Zong YY, Xu TL, Zhang GY. Neuroprotection against ischemic brain injury by a small peptide inhibitor of c-Jun N-terminal kinase (JNK) via nuclear and non-nuclear pathways. *Neuroscience*. 2006;139(2):609–627.
50. Mason JM. Design and development of peptides and peptide mimetics as antagonists for therapeutic intervention. *Future Med Chem*. 2010;2(12):1813–1822.
51. Kurzawa L, Pellerano M, Morris MC. PEP and CADY-mediated delivery of fluorescent peptides and proteins into living cells. *Biochim Biophys Acta*. 2010;1798(12):2274–2285.
52. Bailey JA, Lahiri DK. A novel effect of rivastigmine on pre-synaptic proteins and neuronal viability in a neurodegeneration model of fetal rat primary cortical cultures and its implication in Alzheimer's disease. *J Neurochem*. 2010;112(4):843–853.
53. Bisht S, Khan MA, Bekhit M, et al. A polymeric nanoparticle formulation of curcumin (NanoCurc) ameliorates CCl4-induced hepatic injury and fibrosis through reduction of pro-inflammatory cytokines and stellate cell activation. *Lab Invest*. 2011;91(9): 1383–1395.
54. Ray B, Bisht S, Maitra A, Maitra A, Lahiri DK. Neuroprotective and neurorescue effects of a novel polymeric nanoparticle formulation of curcumin (NanoCurc™) in the neuronal cell culture and animal model: implications for Alzheimer's disease. *J Alzheimers Dis*. 2011;23(1):61–77.
55. Zhang YH, Mann D, Raymick J, Sarkar S, Paule MG, Lahiri DK, Dumas M, Bell-Cohen A, Schmued LC. K114 inhibits A-beta aggregation and inflammation in vitro and in vivo in AD/Tg mice. *Curr Alzheimer Res*. 2014;11(3):299–308.
56. Hinkerohe D, Smikalla D, Schoebel A, et al. Dexamethasone prevents LPS-induced microglial activation and astroglial impairment in an experimental bacterial meningitis co-culture model. *Brain Res*. 2010;1329:45–54.
57. Figuera-Losada M, Rojas C, Slusher BS. Inhibition of microglia activation as a phenotypic assay in early drug discovery. *J Biomol Screen*. 2014;19(1):17–31.
58. Srinivasan M, Lu D, Eri R, et al. CD80 binding polyproline helical peptide inhibits T cell activation. *J Biol Chem*. 2005;280(11): 10149–10155.
59. Srinivasan M, Srihari J. Glucocorticoid induced leucine zipper mimic inhibits experimental autoimmune encephalomyelitis. *J Immunol*. 2012;188 (Meeting Abstract Supplement):Abstract 119.7.
60. Ray B, Lahiri DK. Neuroinflammation in Alzheimer's disease: different molecular targets and potential therapeutic agents including curcumin. *Curr Opin Pharmacol*. 2009;9(4):434–444.

Drug Design, Development and Therapy Dovepress

Publish your work in this journal

Drug Design, Development and Therapy is an international, peer-reviewed open-access journal that spans the spectrum of drug design and development through to clinical applications. Clinical outcomes, patient safety, and programs for the development and effective, safe, and sustained use of medicines are a feature of the journal, which has also been accepted for indexing on PubMed Central. The manuscript management system is completely online and includes a very quick and fair peer-review system, which is all easy to use. Visit http://www.dovepress.com/testimonials.php to read real quotes from published authors.

Submit your manuscript here: http://www.dovepress.com/drug-design-development-and-therapy-journal